# Supporting Information

## Holguera et al. 10.1073/pnas.1203824109

### SI Materials and Methods

**Plasmid Constructions.** All plasmids used are listed in Table S3. *Gene 6*, *gene 3*, and the mutant variant p6ΔN13 were amplified by PCR from ϕ29 genomic DNA using the primer sets p6 R-BamHI H33 and p6 L-AatII H33, p3 R-BamHI H33 and p3 L-AatII H33, p6 R-13 BamHI H33 and p6 L-AatII H33, respectively (Table S4). The PCR products obtained were digested with restriction enzymes BamHI and AatII and cloned into the episomal vector pNDH33 digested with the same enzymes. In the resulting constructions, named pNDH33-p6, pNDH33-p3, and pNDH33-p6ΔN13, respectively, the indicated PCR products were located behind the isopropyl β-D-1-thiogalactopyranoside (IPTG)-inducible promoter $P_{grac}$. Later, these vectors were used to transform competent *Bacillus subtilis* cells. To obtain *spo0A* deletion strains, chloramphenicol-resistant transformants were selected and transformed de novo with chromosomal DNA ($Km^R$) from the SWV215 *B. subtilis* strain. To obtain p6R6A, p6R6A-c-Myc, and TP-S232T mutants, plasmids pNDH33-p6, pNDH33-p6-c-Myc, and pNDH33-p3 were used as templates for site-directed mutagenesis with oligonucleotides p6 R-R6A and p6 L-R6A or p3S232T-R and p3S232T-L. To construct the C-terminal c-Myc-tagged protein p6, ϕ29 *gene 6* was amplified by PCR using oligonucleotides p6pMUTIN-cMyc-R KpnI and p6pMUTIN-cMyc-L EagI (which introduced the KpnI and EagI restriction sites) and cloned into the pMUTIN-c-Myc vector digested with the same enzymes. Then, the *gene p6-c-Myc* fusion was isolated from the pMUTIN-p6-c-Myc vector by PCR using primers p6BamHI c-Myc-R and p6AatII c-Myc-L (which introduced the restriction sites BamHI and AatII). This construction was subsequently cloned into the vector pNDH33, digested with the same enzymes. To obtain the p6ΔN13-c-Myc mutant, fragment p6ΔN13-c-Myc was amplified by PCR with the primer set p6 R-13 BamHI H33 and p6 L-AatII H33-c-Myc, using plasmid pNDH33-p6-c-Myc as template, and cloned into pNDH33 vector digested with enzymes BamHI and AatII. All constructs were verified by DNA sequencing.

The ectopically expressed c-Myc-tagged protein p6 was shown to be functional by complementation experiments using the replication-deficient phage *sus6*(626) (Fig. S6).

**Analysis of p6 Accumulation by Western Blotting.** *B. subtilis* strains 110NA and IH-04 were grown at 37 °C in Luria–Bertani (LB) medium supplemented with 5 mM $MgSO_4$. At an $OD_{600}$ of 0.45–0.5, cultures were split into two aliquots. One of the IH-04 aliquots was induced with 1 mM IPTG and the other one was kept uninduced. In the case of 110NA, one of the aliquots was infected with wild-type phage ϕ29 at a multiplicity of infection (MOI) of 5 and the other one was kept uninfected. Samples of 1.5 mL were taken at the indicated times post induction or post infection, respectively, and pellets were resuspended in a final volume of 250 μL of loading buffer [37 mM Tris·HCl (pH 6.8), 2% (wt/vol) SDS, 4% (vol/vol) β-mercaptoethanol, and 13% (vol/vol) glycerol] and disrupted by sonication. Samples were then loaded onto a 16% (wt/vol) polyacrylamide Tris-tricine gel and separated by electrophoresis before transference to polyvinylidene difluoride membranes (Immobilon-P, Millipore) by electroblotting. As a control, 50 ng of purified protein p6 was run in the same gel. Membrane was probed with 1:3,000-diluted rat anti-p6 polyclonal antibodies for 1 h at room temperature. Then, membranes were washed four times with PBS-0.05% Tween 20 and incubated with 1:4,000-diluted anti-rat horseradish peroxidase-conjugated antibodies, for 1 h at room temperature. Detection of immune complexes was carried out with an ECL kit (Amersham). Rat anti-p6 antibodies were affinity-purified using Hi-Trap NHS-activated HP columns (GE Healthcare).

**RNA Isolation, RT-quantitative PCR, and Data Analysis.** *B. subtilis* strains IH-02 (control sample) and IH-04 (expressing p6) were grown at 37 °C in LB medium supplemented with 5 mM $MgSO_4$ to early exponential phase. At an $OD_{600}$ of 0.3–0.35, IPTG was added to the medium to a final concentration of 1 mM. Samples (1 mL) were harvested 30 min later, and total RNA was immediately extracted using the MasterPure RNA Purification Kit (Epicentre) according to the manufacturer's recommendations. The quality and quantity of total RNA were determined by Nanodrop ND-1000 UV spectroscopy (Thermo Scientific), and RNA integrity was checked using a 2100 Bioanalyzer (Agilent Technologies). Reverse transcription of RNA was performed using the High Capacity RNA-to-cDNA Master Mix (Applied Biosystems PN4390712) according to the manufacturer's instructions using 500 ng of total RNA. Negative RT controls were included for each reaction. PCR primers for RT-quantitative PCR (qPCR) (Table S4) were designed using AmplifX 1.5.4 software. The specificity of primer pairs was assessed in silico by matching them against the complete 168 *B. subtilis* genome. PCR efficiency for each primer pair was calculated using fourfold dilutions (from 50 ng) of pooled cDNA. qPCR reactions were performed on a BioRad CFX 384 instrument in a 10-μL final reaction volume with 5 ng of cDNA, 2.5 μM of each forward and reverse primer, and 5 μL of Power Sybr Green reaction mix (Applied Biosystems). Cycling parameters were as follows: 10 min at 95 °C followed by 40 two-step cycles of 95 °C for 15 s + 64 °C for 30 s. Melting curve analysis from 60 °C to 95 °C (0.5 °C/s) was included at the end of the program. No-template controls were always negative.

To identify the most stably expressed gene, the expression values of all genes were processed in the application NormFinder (1). The *polC* gene was identified as the most stably expressed gene and was used as the reference gene to normalize Ct values. For each strain, RNA samples were extracted from three independent cultures, and each sample was loaded in triplicate on the qPCR plate. Changes in mRNA levels were calculated using the $2^{-\Delta\Delta}$CT method (2). Statistical analysis was performed using software GeneEx 5.3.6.170. Data were analyzed by Mann–Whitney *U* test, applying Dunn–Bonferroni correction. Results with *P* values <0.00639 were considered statistically significant.

**Image Acquisition and Image Analysis.** Image acquisition was performed using a C9100-02 CCD camera (Hamamatsu) attached to a Zeiss Axiovert 200M microscope. The digital images were acquired and analyzed with METAMORPH version 7.1.2.0 software. Images of fluorescent samples were deconvolved within METAMORPH and assembled in Adobe PHOTOSHOP CS4 version 11.0.2.

**Immunofluorescence Microscopy.** Affinity-purified rat and rabbit polyclonal antibodies against p6 and p3, respectively, were used at a dilution of 1:1,000, and incubations were carried out for 1 h at room temperature. Polyclonal antibodies were centrifuged for 10 min at 14,000 × *g* at 4 °C before use to precipitate possible antibody aggregates. The monoclonal antibodies mouse anti-c-Myc and mouse anti–5-bromo-2′-deoxyuridine (BrdU) were used at 1:1,000 and 1:100 dilutions, respectively, and incubated for 1 h at room temperature. Alexa Fluor 488-conjugated (Invitrogen) anti-rat and anti-mouse antibodies were used at a 1:1,000 dilu-

tion and incubated at 4 °C overnight. Alexa Fluor 594-conjugated (Invitrogen) anti-rat and anti-rabbit antibodies were used at a dilution of 1:1,000 and incubated at 4 °C overnight. These and all subsequent steps were performed with minimal exposure of the samples to light. All samples were mounted for epifluorescence microscopy in multispot microscope slides (C. A. Hendley, Loughton, England) supplemented with 0.2 μg/mL DAPI.

1. Andersen CL, Jensen JL, Ørntoft TF (2004) Normalization of real-time quantitative reverse transcription-PCR data: A model-based variance estimation approach to identify genes suited for normalization, applied to bladder and colon cancer data sets. *Cancer Res* 64:5245–5250.

2. Livak KJ, Schmittgen TD (2001) Analysis of relative gene expression data using real-time quantitative PCR and the 2(-Delta Delta C(T)) Method. *Methods* 25:402–408.

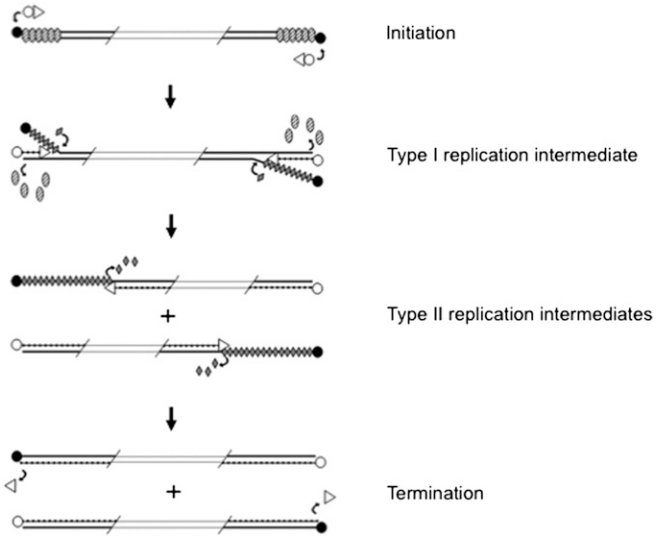


**Fig. S1.** Mechanism of in vitro ϕ29 DNA replication. Replication starts by recognition of the p6-nucleoprotein complexed origins of replication by a terminal protein (TP)/DNA polymerase heterodimer. The DNA polymerase then catalyzes the addition of the first dAMP to the TP present in the heterodimer complex. After a transition step, these two proteins dissociate, and the DNA polymerase continues processive elongation that is coupled to strand displacement. The ϕ29-encoded SSB protein p5 binds to the displaced ssDNA strands and is removed by the DNA polymerase during later stages of the replication process. Continuous elongation of the DNA polymerase from both DNA ends generates replication intermediates that finally converge in the complete duplication of the parental strands. Circles, TP; triangles, DNA polymerase; ovals, replication initiator protein p6; diamonds, SSB protein p5; de novo synthesized DNA is shown as beads on a string.

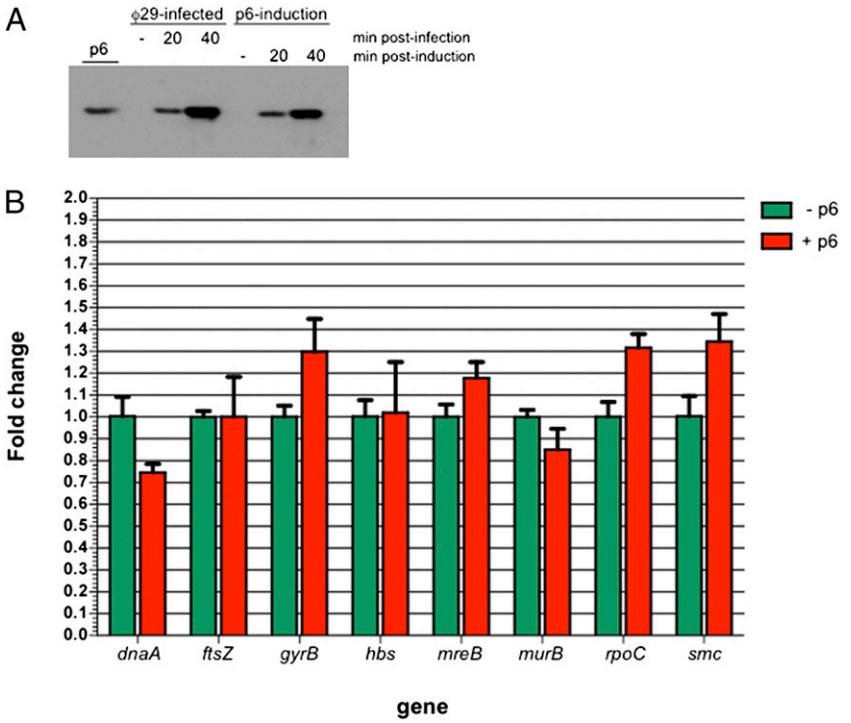


**Fig. S2.** Expression of protein p6 does not affect *B. subtilis* DNA transcription. (*A*) Samples of 1.5 mL from infected and noninfected 110NA cultures, and from IPTG-induced and noninduced cultures of strain IH-04, were taken at the indicated times post infection or post induction, respectively, and analyzed by Western Blotting using antibodies against p6. (*B*) Relative expression of the genes indicated in *B. subtilis* strains IH-02 (control sample) and IH-04 (expressing p6) induced with IPTG and measured by RT-qPCR assay. Transcript levels of genes were normalized to the level of the *polC* gene and compared with control samples. Data represent mean ± SD. *dnaA*: $P = 0.0808$; *ftsZ*: $P = 1$; *gyrB*: $P = 0.0808$; *hbs*: $P = 1$; *mreB*: $P = 0.0808$; *murB*: $P = 0.0808$; *rpoC*: $P = 0.0808$; and *smc*: $P = 0.0808$.

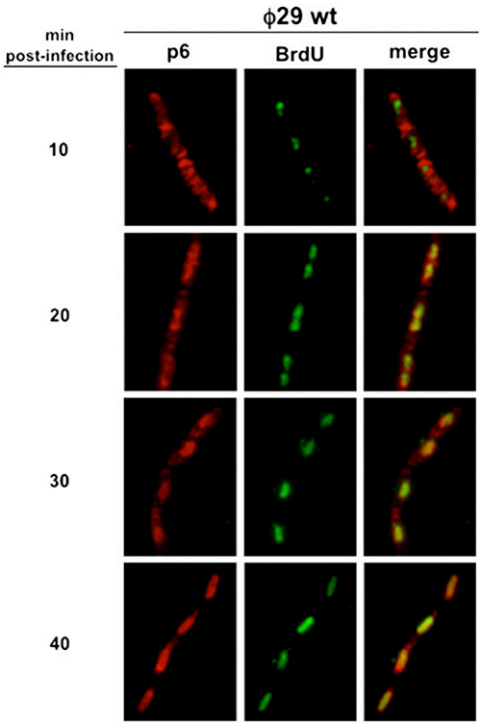


**Fig. S3.** Colocalization of ϕ29 dsDNA and protein p6 during the viral cycle. *B. subtilis* strain 110NA was grown at 37 °C in LB medium supplemented with 5 mM $MgSO_4$. At an $OD_{600}$ of 0.45–0.5, cells were infected with wild-type phage ϕ29 at a MOI of 5, and 75 μM HpUra was added to the medium. For viral DNA labeling, BrdU was added to the culture 3 min post infection, and samples were harvested at the indicated times after infection and processed for immunodetection using polyclonal antibodies against p6. For clarity, p6 and DAPI fluorescent signals are false-colored red and green, respectively.

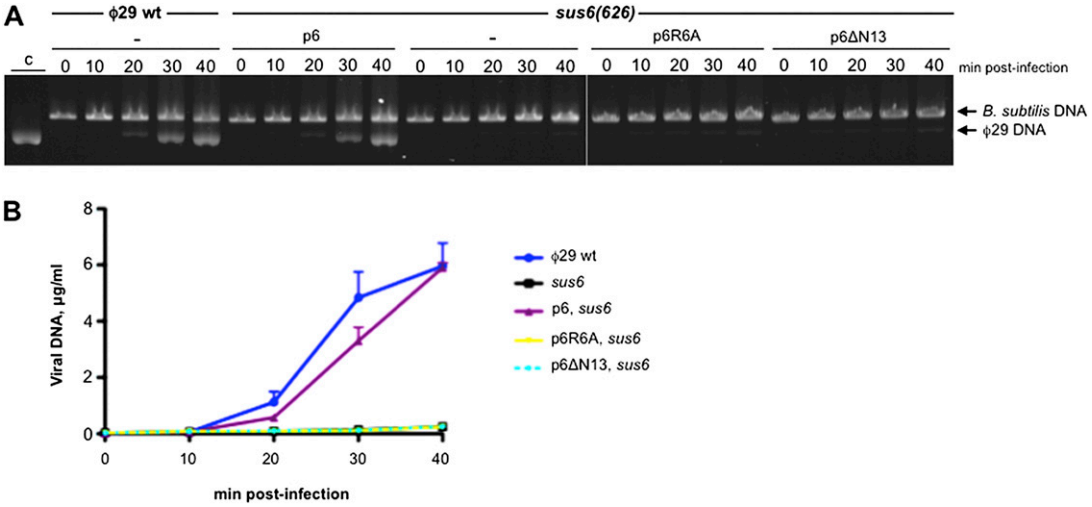


**Fig. S4.** ϕ29 DNA replication is impaired in DNA-binding mutants p6R6A and p6ΔN13. (*A*) Agarose gel electrophoresis analysis showing the amount of viral DNA (in micrograms of viral DNA per milliliter of culture) accumulated in the *B. subtilis* strains IH-04 [expressing p6 wt (wild-type)], IH-06 (expressing p6R6A mutant), and IH-08 (expressing p6ΔN13 mutant) at different times after infection with the *sus6*(626) mutant phage. As an internal control, *B. subtilis* 168 Δ*spo0A* strain was infected with either ϕ29 wild-type or *sus6*(626) mutant phage, and the production of viral DNA was analyzed at the indicated times post infection. Arrows indicate positioning of the ϕ29 genome and *B. subtilis* chromosomal DNA. (*B*) The amount of intracellular accumulated phage ϕ29 DNA in the strains indicated above was quantified by real-time PCR. Mean and SEM values were derived from three independent experiments.

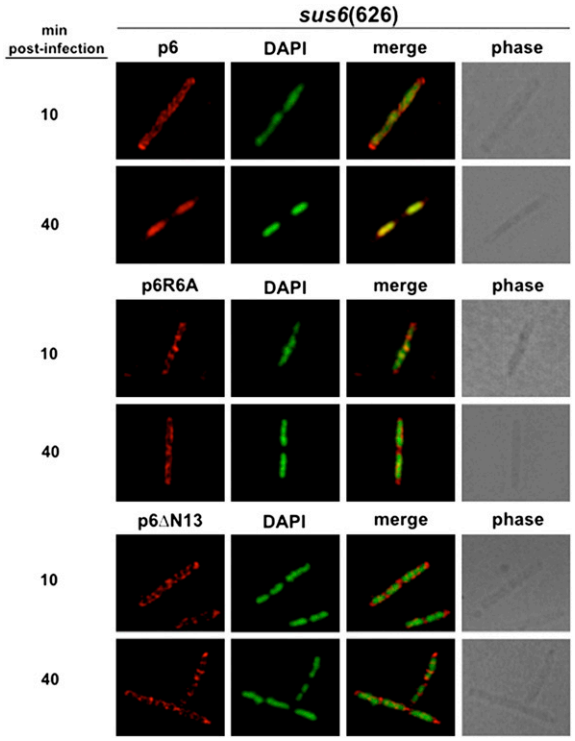


**Fig. S5.** Protein p6 mutants in DNA-binding capacity are not distributed at the bacterial nucleoid in the absence of viral DNA replication. *B. subtilis* strains IH-04 (expressing p6 wild-type), IH-06 (expressing p6R6A), and IH-08 (expressing p6ΔN13) were grown at 37 °C in LB medium containing 5 mM $MgSO_4$. At an $OD_{600}$ of 0.45–0.5, cells were infected with *sus6*(626) mutant phage at a MOI of 5, and 1 mM IPTG was added to the medium. Samples were withdrawn at the indicated times post infection and subjected to immunofluorescence microscopy using polyclonal antibodies against p6. For clarity, p6 and DAPI fluorescent signals are false-colored red and green, respectively.

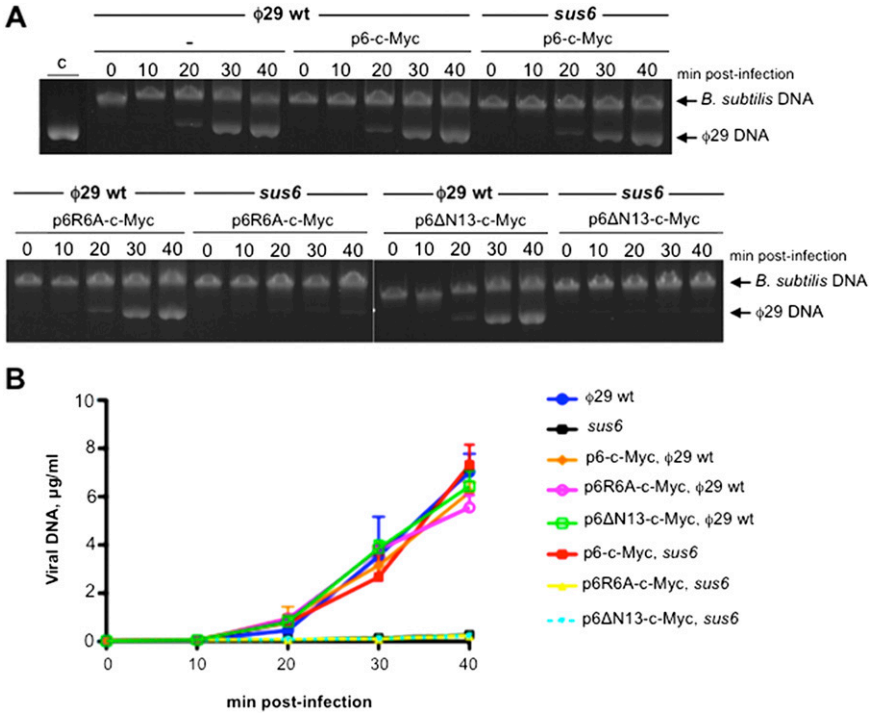


**Fig. S6.** Protein p6-c-Myc is functional in vivo. (*A* and *B*) Complementation experiments using wild-type phage ϕ29 or *sus6*(626) mutant phage infecting strains IH-10 (expressing p6-c-Myc), IH-12 (expressing p6R6A-c-Myc), or IH-14 (expressing p6ΔN13-c-Myc). As an internal control, *B. subtilis* 168 Δ*spo0A* strain was infected with either ϕ29 wild-type or *sus6*(626) mutant phage, and the production of viral DNA was analyzed at the indicated times post infection. (*A*) Agarose gel electrophoresis analysis illustrating the amount of viral DNA accumulated in the strains indicated above at different times post infection. Arrows indicate positioning of the ϕ29 genome and *B. subtilis* chromosomal DNA. (*B*) The amount of intracellular accumulated viral DNA was quantified by real-time PCR. Mean and SEM values were derived from three independent experiments.

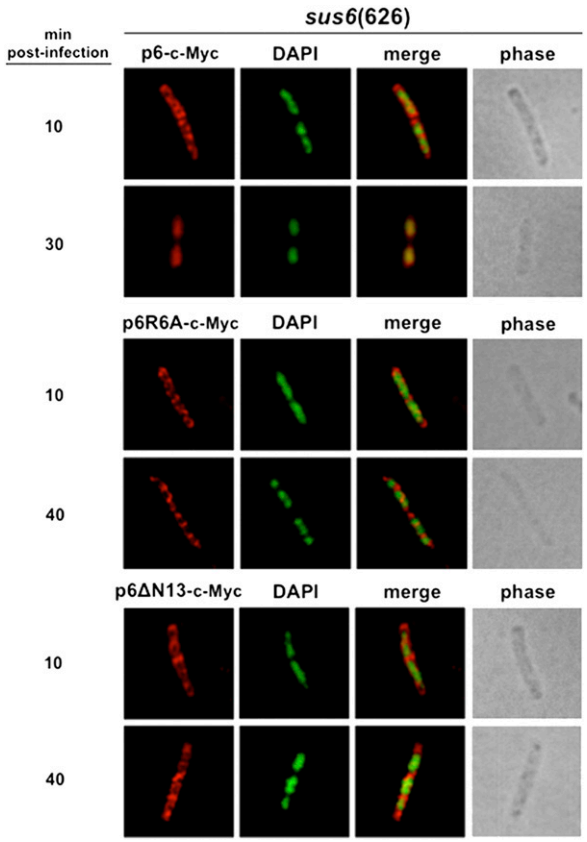


**Fig. S7.** Protein p6-cMyc is efficiently distributed at the bacterial nucleoid. Strains IH-10 (expressing p6-c-Myc), IH-12 (expressing p6R6A-c-Myc), and IH-14 (expressing p6ΔN13-cMyc) were grown at 37 °C in LB medium containing 5 mM $MgSO_4$. At an $OD_{600}$ of 0.45–0.5, cells were infected with *sus6*(626) mutant phage at a MOI of 5, and 50 μM IPTG was added to the medium. Samples were withdrawn at the indicated times post infection and subjected to immunofluorescence microscopy using polyclonal antibodies against p6. For clarity, p6 and DAPI fluorescent signals are false-colored red and green, respectively.

**Table S1. ϕ29 phages used**

| Phage | Source or reference |
|---|---|
| ϕ29 wild-type | Laboratory stock |
| *sus2(513)* | Moreno et al. (1) |
| *sus3(91)* | Moreno et al. (1) |
| *sus6(626)* | Reilly et al. (2) |

1. Moreno F, Camacho A, Viñuela E, Salas M (1974) Suppressor-sensitive mutants and genetic map of *Bacillus subtilis* bacteriophage ϕ29. *Virology* 62(1):1–16.
2. Reilly BE, Zeece VM, Anderson DL (1973) Genetic study of suppressor-sensitive mutants of the *Bacillus subtilis* bacteriophage ϕ29. *J Virol* 11:756–760.

**Table S2. Strains used**

| Strain | Relevant genotype | Construction, source, or reference |
|---|---|---|
| *E. coli* | | |
| XL1-blue | *rec*A1, *end*A1, *gyr*A96, *thi*-1, *hsd*R17($r_K-$, $m_K+$), *sup*E44, *rel*A1, *lac*, [F′, *proAB*, *lac*I$^q$ZΔM15::Tn10(tet$^r$)] | Laboratory stock |
| *B. subtilis* | | |
| 110NA | *trpC2 spo0A3 su*$^-$ | Moreno et al. (1) |
| 168 | *trpC2*, considered wild-type strain | BGSC* |
| 168 Δspo0A | *trpC2 Ω(spo0A::kan)* | SWV215 → 168 ($K_m$) |
| SWV215 | *trpC2 pheA1 Ω(spo0A::kan)* | Xu and Strauch (2) |
| IH-01 | *trpC2* $P_{grac}$ *cat* | pNDH33 → 168 (Cm) |
| IH-02 | *trpC2* $P_{grac}$*-cat Ω(spo0A::kan)* | SWV215 → IH-01 ($K_m$) |
| IH-03 | *trpC2* $P_{grac}$*-p6 cat* | pNDH33-p6 → 168 (Cm) |
| IH-04 | *trpC2* $P_{grac}$*-p6 cat Ω(spo0A::kan)* | SWV215 → IH-03 ($K_m$) |
| IH-05 | *trpC2* $P_{grac}$*-p6R6A cat* | pNDH33-p6R6A → 168 (Cm) |
| IH-06 | *trpC2* $P_{grac}$*-p6R6A cat Ω(spo0A::kan)* | SWV215 → IH-05 ($K_m$) |
| IH-07 | *trpC2* $P_{grac}$*-p6ΔN13 cat* | pNDH33-p6ΔN13 → 168 (Cm) |
| IH-08 | *trpC2* $P_{grac}$*-p6ΔN13 cat Ω(spo0A::kan)* | SWV215 → IH-07 ($K_m$) |
| IH-09 | *trpC2* $P_{grac}$*-p6c-Myc cat* | pNDH33-p6-c-Myc → 168 (Cm) |
| IH-10 | *trpC2* $P_{grac}$*-p6c-Myc cat Ω(spo0A::kan)* | SWV215 → IH-09 ($K_m$) |
| IH-11 | *trpC2* $P_{grac}$*-p6R6Ac-Myc cat* | pNDH33-p6R6A-c-Myc → 168 (Cm) |
| IH-12 | *trpC2* $P_{grac}$*-p6R6Ac-Myc cat Ω(spo0A::kan)* | SWV215 → IH-11 ($K_m$) |
| IH-13 | *trpC2* $P_{grac}$*-p6ΔN13c-Myc cat* | pNDH33-p6ΔN13-c-Myc → 168 (Cm) |
| IH-14 | *trpC2* $P_{grac}$*-p6ΔN13c-Myc cat Ω(spo0A::kan)* | SWV215 → IH-13 ($K_m$) |
| IH-15 | *trpC2* $P_{grac}$*-p3 cat* | pNDH33-p3 → 168 (Cm) |
| IH-16 | *trpC2* $P_{grac}$*-p3 cat Ω(spo0A::kan)* | SWV215 → IH-15 ($K_m$) |
| IH-17 | *trpC2* $P_{grac}$*-p3S232T cat* | pNDH33-p3S232T → 168 (Cm) |
| IH-18 | *trpC2* $P_{grac}$*-p3S232T cat Ω(spo0A::kan)* | SWV215 → IH-17 ($K_m$) |
| IH-19 | *trpC2* $P_{grac}$*-p3 cat + pPR55w6 phleo* | pPR55w6 → IH-15 (Pm) |

Antibiotic resistance gene abbreviations are as follows: cat, chloramphenicol; kan, kanamycin; phleo, phleomycin. "X" → "Y" indicates that "strain Y" was transformed with DNA from "source X," with the selected marker in parentheses. Cm, chloramphenicol; $K_m$, kanamycin; Pm, phleomycin.
**Bacillus* Genetic Stock Center.


1. Moreno F, Camacho A, Viñuela E, Salas M (1974) Suppressor-sensitive mutants and genetic map of *Bacillus subtilis* bacteriophage ϕ29. *Virology* 62(1):1–16.
2. Xu K, Strauch MA (1996) Identification, sequence, and expression of the gene encoding gamma-glutamyltranspeptidase in *Bacillus subtilis*. *J Bacteriol* 178:4319–4322.


**Table S3. Plasmids used**

| Plasmids | Relevant features | Reference |
|---|---|---|
| pNDH33 | $P_{grac}$-cat | Phan et al. (1) |
| pMUTIN-c-Myc | *bla* $P_{spac}$, C-terminal c-Myc fusion vector | Kaltwasser et al. (2) |
| pMUTIN-p6-c-Myc | pMUTIN-c-Myc containing ϕ29 *gene 6* | This work |
| pNDH33-p6 | pNDH33 containing ϕ29 *gene 6* | This work |
| pNDH33-p6R6A | pNDH33 containing ϕ29 mutant *gene 6-R6A* | This work |
| pNDH33-p6ΔN13 | pNDH33 containing ϕ29 mutant *gene 6-ΔN13* | This work |
| pNDH33-p6-c-Myc | pNDH33 containing ϕ29 *gene 6-c-Myc C-terminal fusion* | This work |
| pNDH33-p6R6A-c-Myc | pNDH33 containing ϕ29 mutant *gene 6-R6A-c-Myc C-terminal fusion* | This work |
| pNDH33-p6ΔN13-c-Myc | pNDH33 containing ϕ29 mutant *gene 6-ΔN13-c-Myc C-terminal fusion* | This work |
| pNDH33-p3 | pNDH33 containing ϕ29 *gene 3* | This work |
| pNDH33-p3S232T | pNDH33 containing ϕ29 mutant *gene 3-S232T* | This work |
| pPR55w6 | pPR55 containing ϕ29 *gene 6* | Bravo et al. (3) |


1. Phan TTP, Nguyen HD, Schumann W (2006) Novel plasmid-based expression vectors for intra- and extracellular production of recombinant proteins in *Bacillus subtilis*. *Protein Expr Purif* 46(2):189–195.
2. Kaltwasser M, Wiegert T, Schumann W (2002) Construction and application of epitope- and green fluorescent protein-tagging integration vectors for *Bacillus subtilis*. *Appl Environ Microbiol* 68:2624–2628.
3. Bravo A, Hermoso JM, Salas M (1994) A genetic approach to the identification of functional amino acids in protein p6 of *Bacillus subtilis* phage ϕ29. *Mol Gen Genet* 245:529–536.

**Table S4. Oligonucleotides used**

| Oligonucleotide | Sequence |
|---|---|
| p6pMUTIN-cMyc-R KpnI | 5′-gag tct aca aat agg tac cga aag tgg gac gaa gaa atg gc-3′ |
| p6pMUTIN-cMyc-L EagI | 5′-cct tct ctt gtg ttt cgg ccg ttc agc aac ctg ttc ttc tgg-3′ |
| p6BamHI c-Myc-R | 5′-ccg aaa gtg gga cgg atc cat ggc aaa aat gat gca gag-3′ |
| p6AatII c-Myc-L | 5′-ggc ggg ctg cga cgt ctt att aaa gat ctt ctt cgc-3′ |
| p6 R-BamHI H33 | 5′-gtg gga cgg atc cat ggc aaa aat gat gca g-3′ |
| p6 L-AatII H33 | 5′-ctt gtg gac gtc tca ttc agc aac ctg ttc ttc-3′ |
| p6 R-13 BamHI H33 | 5′-cac aaa ggg atc cat gaa cgt tgc caa aat ggt g-3′ |
| p6 L-AatII H33-c-Myc | 5′-ggc tgc ccc ggg gac gtc tta tta aag atc-3′ |
| p6 R-R6A | 5′-cca tgg caa aaa tga tgc agg cag aaa tca caa aga caa ccg-3′ |
| p6 L-R6A | 5′-cgg ttg tct ttg tga ttt ctg cct gca tca ttt ttg cca tgg-3′ |
| p3 R-BamHI H33 | 5′-gat aag gat cca tgg cga gaa gtc cac g-3′ |
| p3 L-AatII H33 | 5′-ctt taa gac gtc cta gaa ccc ctt taa gct tag-3′ |
| p3S232T-R | 5′-cct ttg agg aat ttg ata ctg agg gaa aca cag tgg ag-3′ |
| p3S232T-L | 5′-ctc cac tgt gtt tcc ctc agt atc aaa ttc ctc aaa gg-3′ |
| R-OUT-SUPER | 5′-aaa tag att ttc ttt ctt ggc tac-3′ |
| R-25 | 5′-aaa gta ggg tac agc gac aac ata c-3′ |
| dnaA-R | 5′-tta gcg ggg aaa gaa caa acc ca-3′ |
| dnaA-L | 5′-gtg agc gca atc tgt ctt caa gtg-3′ |
| ftsZ-R | 5′-cag tga ttg caa ccg gct tta tcg-3′ |
| ftsZ-L | 5′-ttt tgg ctc acg ctt cgg aac a-3′ |
| gyrB-R | 5′-ctg cag cgt tac aaa ggt ctt ggt-3′ |
| gyrB-L | 5′-agt ctc atc cgc atc cat tgc atc-3′ |
| hbs-R | 5′-ggt tgc aga agc aag cga att gtc-3′ |
| hbs-L | 5′-gaa cgt tca cgc acc tcg aag tta-3′ |
| mreB-R | 5′-gac cgt acg gct gaa gcg att aaa-3′ |
| mreB-L | 5′-ggc aaa cct gtg agc aaa tcg c-3′ |
| murB-R | 5′-tgc agc ttg agc aga agg ata agg-3′ |
| murB-L | 5′-ggc atg att cgg aag cgg att tct-3′ |
| polC-R | 5′-gtt tgt cct gag tgc cag cat tct-3′ |
| polC-L | 5′-ttc cgc aat gag ggc atg tct t-3′ |
| rpoC-R | 5′-acc gta tgc agg gtg ttg aaa tcg-3′ |
| rpoC-L | 5′-aca tca gtg tca ccg gca tca atc-3′ |
| smc-R | 5′-atc agc gca tca agc ttc agc a-3′ |
| smc-L | 5′-caa gct cga ctt cca ttc gtc caa-3′ |